

Characterisation of radio frequency heating systems in industry using a network analyser

R.I. Neophytou
A.C. Metaxas

Indexing terms: Radio frequency heating systems, Network analyser

Abstract: The authors describe a rapid method for attaining the desired electrical condition which matches a loaded applicator to the tank circuit of a high power radio frequency source. First, the circuit equations of two coupled resonant circuits are derived and used to predict the optimum matching conditions with respect to various criteria. These conditions are then studied experimentally using an automatic network analyser which is coupled to the applicator/tank circuit assembly via a small launching coil. The analysis considers the interaction of this launching coil with the tank circuit only; and with both the tank circuit and the applicator. The key parameters used to identify optimum matching conditions are the values of the two return loss responses and, specifically, their interrelation, as observed on the network analyser. Finally, an example is given of matching a particular radio frequency system using the present experimental method. The results are in good agreement with those from the more accurate, but extremely elaborate, nonlinear minimisation procedure.

List of principal symbols

C_1, C_2	tank and applicator capacitances
C_{12}	equivalent capacitance of tank and applicator circuits combined
D	return loss
D_{min_1}, D_{min_2}	values of minima of return loss D
E_0	voltage source driving tank and applicator circuits
f_0	operating frequency
f_1, f_2	tank and applicator resonant frequencies
f_{min_1}, f_{min_2}	frequencies of minima of return loss D
I_1, I_2	tank and applicator currents
k, k_1, k_2	coupling factors, tank-applicator, launching coil-tank and launching coil-applicator

L_1, L_2	tank and applicator inductances
L_{12}	equivalent inductance of tank and applicator circuits combined
L_l	launching coil inductance
M, M_1, M_2	mutual inductances, tank-applicator, launching coil-tank and launching coil-applicator
P_{in}	input power to tank circuit
P_{out}	output power to load
Q_1, Q_2	tank and applicator Q-factors
R_1, R_2	tank and applicator resistances
R_{12}	equivalent resistance of tank and applicator circuits combined
R_l	launching coil resistance
X_1, X_2	tank and applicator reactances
Z_1, Z_2	tank and applicator impedances
Z_{12}	equivalent impedance of tank and applicator circuits combined referred to tank
Z_{NA}	impedance seen by network analyser
η	power transfer efficiency from tank to applicator circuit
ρ	reflection coefficient
ω_0	angular operating frequency
ω_1, ω_2	tank and applicator angular resonant frequencies

1 Introduction

Radio frequency (RF) heating in industry, at 13.56 MHz and 27.12 MHz, is an established technique for processing various materials [1, 2]. Applications range from drying of textiles to moisture levelling of biscuits and from the welding of plastics to the heating of woollen bales. The annual equipment sales, typically in the range 40–200 kW per installation, are estimated at around 30 million pounds sterling per annum worldwide with plastics welding commanding a good proportion of the total.

There are two basic technologies which characterise the design of equipment in this industry [2]. Self-excited oscillators, operating under class C conditions, represent over 99% of the equipment operating in industry, while the 50 Ω technology, employing a crystal oscillator with subsequent amplification through a vacuum amplifier, is slowly gaining acceptance despite the increased cost per kW installed. This is primarily because of the 50 Ω technology's superior frequency stability and better compliance with new stringent

© IEE, 1997

IEE Proceedings online no. 19971351

Paper first received 15th November 1996 and in revised form 16th April 1997

The authors are with the Department of Engineering, University of Cambridge, Trumpington Street, Cambridge CB2 1PZ, UK

EMC regulations which are coming into force, particularly in Europe.

The overwhelming majority of the radio frequency processing installations in industry today utilise variants of the basic class C power oscillator. A number of studies have been undertaken in the last decade to examine the operation of these circuits [3] and to ensure that these systems are designed optimally with high efficiency and safety [2]. The most commonly used arrangement for dielectric heating installations are the series and shunt fed self-excited tuned anode oscillator circuits, as shown in Figs. 1a and b, respectively. The tank circuits can take the form of either lumped elements as shown in Fig. 1 or distributed inductance resonant cavities [2]. A recent paper described a computer model which simulates the operation of these circuits using the SABER Simulator written by Analogy Inc. [4]. Using this model estimates for the power efficiency of the class C, combined to the electrical inductive coupling between the tank and applicator circuits, can be obtained.

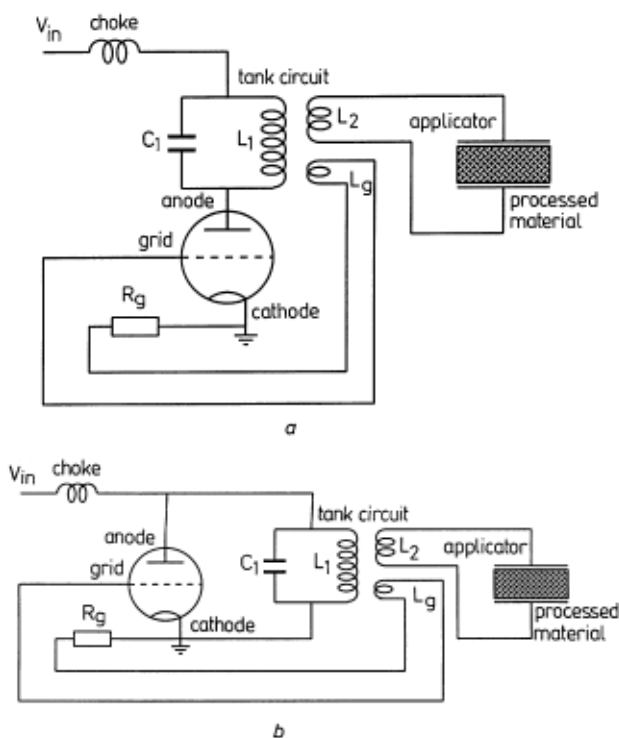


Fig. 1 Self-excited oscillator circuits

Radio frequency measurements are notoriously difficult to perform due to the stray capacitances between the various parts of the applicator and earth and between the applicator and the measuring equipment. It is well recognised that the operator can also cause significant interference unless certain precautions are taken while the measurements are being recorded. In high power operation one starts with the premise that the components comprising the class C circuit have already been chosen to give the highest efficiency, thus leaving the electrode separation of the applicator, once loaded with a material to be processed, to be the only parameter to vary to tune the applicator to the tank circuit.

The single most important advance in recent years in the design of radio frequency processing systems has been the use of an automatic network analyser (NA). Three examples can be cited. First, isolated applicator structures (that is, applicators not connected to the

class C oscillator but containing the material to be processed) were analysed and their frequency responses and Q-factors measured [4, 5]. Secondly, the qualitative interaction between the applicator and the tank oscillatory circuit of the high power unit was investigated [5, 6]. Thirdly, a computer program was used to determine the impedance loci which were displayed on the NA and, by comparing these with experimental results, the various components could be approximately deduced [7].

In this paper the behaviour of the input impedance observed on the NA and in particular the parameters which appear on the return loss response are examined. An interrelation, found among these parameters, determines the coupling factor between the applicator and tank circuits. A new method is then presented which is based on the original network analyser method for the rapid characterisation, at low power, of magnetically coupled circuits. It also takes into account any mutual coupling between the network analyser launching coil and the applicator circuit's inductance. An alternative method to characterise the circuit components is to use a full nonlinear optimisation procedure described in [4]. The method described in this paper avoids this elaborate procedure and, as shown below, gives component values which differ by only up to 11%. The example chosen to validate this analysis considers a typical continuous drying system operating under steady-state conditions. However, this analysis can also be applied to a batch system to characterise it at the beginning of its cycle.

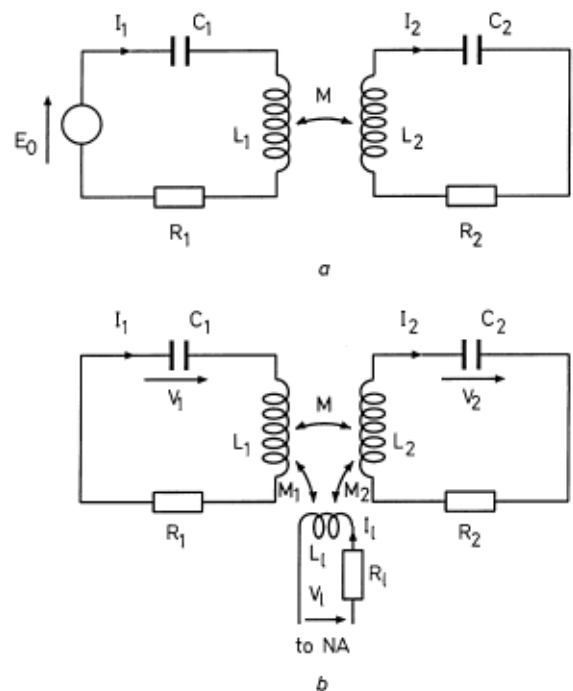


Fig. 2 Equivalent circuit representation of the tank and applicator circuits
a Without launching coil
b With launching coil from the network analyser

2 Coupling between the tank and applicator circuits

The plate separation of the applicator is varied to enable the applicator and tank circuit resonant frequencies to approach each other so that the state of coupling and matching between the two circuits may be assessed. In this paper only the power coupling efficiency is considered. Therefore the vacuum triode and the associ-

ated feedback parts of the circuit can be ignored, reducing the equivalent circuit to that shown in Fig. 2a. An ideal sinusoidal voltage source E_0 of frequency $\omega_0/2\pi$ excites the coupled resonant circuits. The analysis is carried out for the series tank circuit configuration but a similar treatment would apply to parallel resonant circuits.

The equations describing the steady-state forced oscillations of the system shown in Fig. 2a are

$$E_0 = Z_1 I_1 + jM\omega_0 I_2 \quad (1)$$

and

$$0 = Z_2 I_2 + jM\omega_0 I_1 \quad (2)$$

where

$$Z_1 = R_1 + j\left(\omega_0 L_1 - \frac{1}{\omega_0 C_1}\right) = R_1 + jX_1 \quad (3)$$

$$Z_2 = R_2 + j\left(\omega_0 L_2 - \frac{1}{\omega_0 C_2}\right) = R_2 + jX_2 \quad (4)$$

The suffixes 1 and 2 refer to the tank and applicator circuits, respectively. Solving these equations gives an expression for the primary current I_1

$$I_1 = \frac{E_0}{Z_1 + \frac{M^2\omega_0^2}{Z_2}} = \frac{E_0}{Z_{12}} \quad (5)$$

where Z_{12} is the equivalent impedance of the whole system referred to the primary circuit, and is equal to

$$\begin{aligned} Z_{12} &= Z_1 + \frac{M^2\omega_0^2}{Z_2} \\ &= \left[R_1 + \frac{M^2\omega_0^2 R_2}{R_2^2 + X_2^2} \right] + j \left[X_1 - \frac{M^2\omega_0^2 X_2}{R_2^2 + X_2^2} \right] \end{aligned} \quad (6)$$

The secondary current is given by

$$I_2 = \frac{-jM\omega_0 E_0}{Z_1 Z_2 + M^2\omega_0^2} = \frac{-jM\omega_0 E_0}{Z_2 Z_{12}} \quad (7)$$

The circuit is said to be at critical coupling when the following condition is satisfied [8]

$$M^2\omega_0^2 = R_1 R_2 \quad (8)$$

For a coupling less than critical, i.e. $M^2\omega_0^2 < R_1 R_2$, the secondary current has a single maximum with respect to frequency. When the coupling is greater than critical, the secondary current has two maxima whose values are the same for all values of M .

3 Power transfer efficiency conditions

Industrial systems often operate at power levels of 100kW or more, so it is imperative to ensure that their power transfer efficiency is at its maximum possible value. The input power to the tank circuit is given by

$$P_{in} = \text{Re}\{E_0 I_1^*\} \quad (9)$$

The output power to the load is defined as

$$P_{out} = |I_2|^2 R_2 \quad (10)$$

and the power transfer efficiency η is equal to

$$\eta = \frac{P_{out}}{P_{in}} = \frac{\left| \frac{M\omega_0 E_0}{Z_2 Z_{12}} \right|^2 R_2}{\text{Re}\{E_0 I_1^*\}} = \frac{1}{1 + \frac{R_1(R_2^2 + X_2^2)}{M^2\omega_0^2 R_2}} \quad (11)$$

Therefore to have maximum power transfer efficiency we need to minimise the ratio

$$\frac{R_1(R_2^2 + X_2^2)}{M^2\omega_0^2 R_2} \quad (12)$$

By differentiating this ratio with respect to ω_0 and setting it to zero we obtain the condition for maximum power transfer efficiency as

$$\omega_0^2 = \frac{\omega_2^2}{1 - \frac{1}{2Q_2^2}} \quad (13)$$

where ω_2 and Q_2 are the angular resonant frequency and Q-factor of the applicator circuit, respectively.

Given that typically the Q-factor of the secondary circuit, Q_2 , is in the range 10–500 depending on its material loading, the condition for maximum power efficiency is satisfied when the operating frequency is equal to the resonant frequency of the secondary, i.e. $X_2 = 0$. The operating frequency of the oscillator is determined by the impedance as seen from the primary, Z_{12} and the feedback circuit. An expression for the angular frequency of the circuit in Fig. 1a is derived in [8]

$$\begin{aligned} \omega_0^2 &= \frac{1}{L_{12} C_{12}} \left(\frac{r_p + R_{12}}{r_p} \right) \\ &\times \left(\frac{r_g}{r_g + \frac{L_g}{r_p C_{12}} + \frac{L_g R_{12}}{L_{12}} - \frac{M_f^2}{r_p L_{12} C_{12}}} \right) \end{aligned} \quad (14)$$

where r_p is the plate resistance and r_g is the grid resistance of the triode, R_{12} , C_{12} and L_{12} are the equivalent resonant circuit parameters of Z_{12} . Given that r_p and r_g are usually large, the operating frequency is approximately equal to the resonant frequency of the equivalent circuit characterised by the parameters C_{12} and L_{12} . From eqn. 6 the resonant frequency is obtained by setting the imaginary part of Z_{12} to zero

$$X_1 = \frac{M^2\omega_0^2 X_2}{R_2^2 + X_2^2} \quad (15)$$

Since for maximum power efficiency $X_2 = 0$, from eqn. 15 we must have $X_1 = 0$ as well. Therefore the condition for maximum power efficiency operation of an RF system is

$$\omega_0 = \omega_1 = \omega_2 \quad (16)$$

where ω_1 is the resonant frequency of the tank circuit, and the corresponding maximum power efficiency that can be obtained is given by

$$\eta = \frac{1}{1 + \frac{R_1 R_2}{M^2\omega_0^2}} \quad (17)$$

Substituting R_1 , R_2 and M using the coupling factor $k = M/\sqrt{L_1 L_2}$ and the Q-factors and given also that $\omega_0 = \omega_1 = \omega_2$, the expression for the maximum power efficiency is transformed to

$$\eta = \frac{1}{1 + \frac{\omega_1 \omega_2}{\omega_0^2 \frac{M^2}{L_1 L_2} Q_1 Q_2}} = \frac{1}{1 + \frac{1}{k^2 Q_1 Q_2}} \quad (18)$$

Therefore the larger the quantity $k^2 Q_1 Q_2$, the better will be the efficiency.

4 Matching using the network analyser

Having derived the various conditions for maximum power transfer efficiency, the next step is to identify how these operating conditions can be observed using a NA. First, a launching coil of inductance L_l and resistance R_l , connected to the NA, is introduced into the coupled system giving the circuit as shown in Fig. 2b.

In distributed inductance oscillatory tank circuits the launching coil, which is affixed through a small aper-

ture to one of the side walls, usually only interacts with the tank circuit and therefore $M_2 = 0$. However, in lump element tank circuits the launching coil may be placed in such a way that it interacts with both the applicator and the tank circuits. Both cases are analysed in the following Sections.

4.1 Launching coil interacting with the tank circuit only

When $M_2 = 0$ the impedance seen by the NA is given by

$$Z_{NA} = R_l + j\omega L_l + \frac{M_1^2 \omega^2}{Z_{12}} \quad (19)$$

The reflection coefficient ρ is defined as

$$\rho = \frac{Z_{NA} - Z_0}{Z_{NA} + Z_0} \quad (20)$$

where Z_0 is the impedance of the line which is usually 50Ω . The return loss D is defined as

$$D = 20 \log |\rho| \quad (21)$$

What is required is to observe how the reflection coefficient, the return loss and the impedance measured by the NA appear at the optimum operating conditions derived in the previous section. A computer model has been generated using Matlab [10] to calculate and plot these as functions of the circuit parameters. Two cases are considered, when coupling is less, and when it is greater, than critical.

4.1.1 Coupling less than critical: For this case the following results are obtained:

The impedance locus of Z_{NA} as shown on the Smith chart is a single circle which reduces as f_2 gets closer to f_1 , i.e. when optimum matching occurs. Further, when M_1 increases the circle increases in size.

The return loss D has a single minimum. The minimum value decreases as optimum matching is approached. Further, when M_1 increases the peak decreases.

Fig. 3 shows the above effects for a particular system configuration. In this case the resonant frequency of the primary (i.e. the tank circuit) is maintained at 13.56 MHz, one of the ISM allocated frequencies [2].

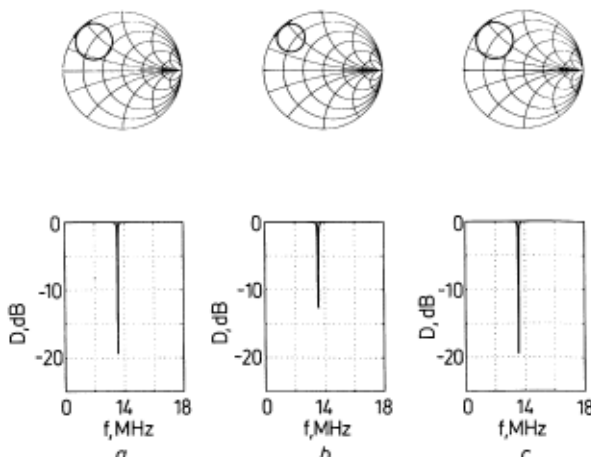


Fig. 3 Impedance loci and return loss D when coupling is less than critical

$f_1 = 13.56\text{MHz}$; $Q_1 = 500$; $L_1 = 1\mu\text{H}$; $Q_2 = 100$; $L_2 = 1\mu\text{H}$; $k^2 Q_1 Q_2 = 0.5$; $k_1 = 0.05$; $k_2 = 0$; $L_l = 0.25\mu\text{H}$

a $f_2 = 12\text{MHz}$
b $f_2 = 13.56\text{MHz}$
c $f_2 = 15\text{MHz}$

4.1.2 Coupling greater than critical: When coupling is greater than critical the following results are

obtained. First, the impedance locus of Z_{NA} consists of two circles, a large one for the tank circuit (high Q) and a small one for the applicator (low Q). As f_2 approaches f_1 the circles tend to become equal in size when optimum matching occurs. Further, the size of each circle increases with M_1 . Secondly, the return loss D has two minima at approximately the resonant frequencies of the two circuits. As f_2 approaches f_1 the minimum associated with the tank circuit is displaced away from f_1 . The minima become closer and nearly equal when optimum matching occurs. Further, when M_1 increases the separation between the two peaks increases. An example of how the impedance locus and the return loss plots change around optimum matching is shown in Fig. 4, once again close to the ISM frequency of 13.56 MHz.

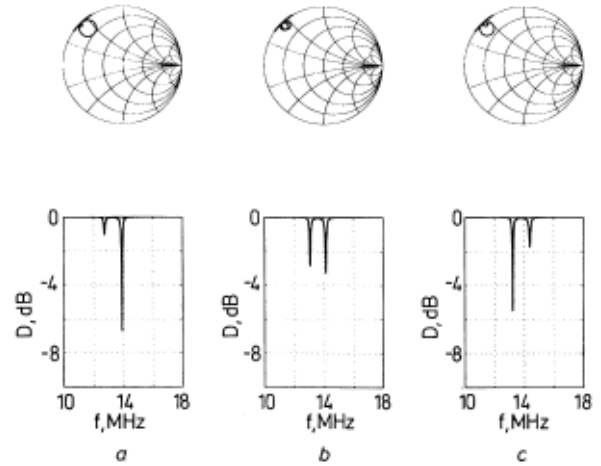


Fig. 4 Impedance loci and return loss D when coupling is greater than critical

$f_1 = 13.56\text{MHz}$; $Q_1 = 500$; $L_1 = 1\mu\text{H}$; $Q_2 = 100$; $L_2 = 1\mu\text{H}$; $k^2 Q_1 Q_2 = 300$; $k_1 = 0.05$; $k_2 = 0$; $L_l = 0.25\mu\text{H}$

a $f_2 = 12\text{MHz}$
b $f_2 = 13.56\text{MHz}$
c $f_2 = 14\text{MHz}$

4.2 Launching coil interacting with both resonant circuits

This is the most general case, when the launching coil is interacting with both resonant circuits, as shown in Fig. 2b. The impedance seen by the NA is now given by (see the Appendix)

$$Z_{NA} = R_l + j\omega L_l + \frac{\omega^2 M_1^2 Z_2 - 2j\omega^3 M_1 M_2 M + \omega^2 M_2^2 Z_1}{\omega^2 M^2 + Z_1 Z_2} \quad (22)$$

To simplify the analysis the model parameters are changed so as to become dimensionless. Therefore the impedance Z_{NA} and subsequently the reflection coefficient ρ and the return loss D become a function of the following circuit parameters:

$$Z_{NA}([f_1, Q_1, L_1], [f_2, Q_2, L_2], [k], [k_1, k_2, L_l]) \quad (23)$$

where $k = M/\sqrt{L_1 L_2}$, $k_1 = M_1/\sqrt{L_1 L_l}$ and $k_2 = M_2/\sqrt{L_2 L_l}$ are the coupling factors for the tank-applicator, launching coil-tank and launching coil-applicator circuits, respectively.

First the effect of L_1 and L_2 is investigated: given that the coupling factors k , k_1 and k_2 are kept constant the computer model shows that the reflection coefficient ρ and the return loss D are independent of the values of L_1 and L_2 . Therefore keeping L_1 and L_2 constant does not affect the general validity of the subsequent results.

We wish to match, using the NA, the applicator circuit to the tank circuit for maximum power transfer efficiency which occurs when the resonant frequencies of the two circuits are equal. This occurrence can be identified by observing how the reflection coefficient ρ or the return loss D changes with the applicator resonant frequency f_2 . The salient features considered here are the positions of the minima of the return loss D and also the values of these minima, as they can be easily measured. The impedance loci are monitored but not investigated in detail as accurate measurements of their radii and positions are much more difficult. Since at most two minima occur, one for each resonant circuit, the notation shown in Fig. 5 is used from now on, where we define the following:

f_{min_1} frequency of first minimum of D

f_{min_2} frequency of second minimum of D ($f_{min_2} > f_{min_1}$)

D_{min_1} value of D at frequency f_{min_1}

D_{min_2} value of D at frequency f_{min_2}

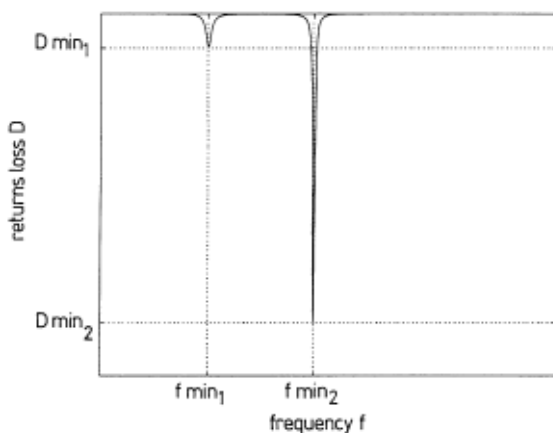


Fig.5 Definition of f_{min_1} , f_{min_2} , D_{min_1} and D_{min_2}

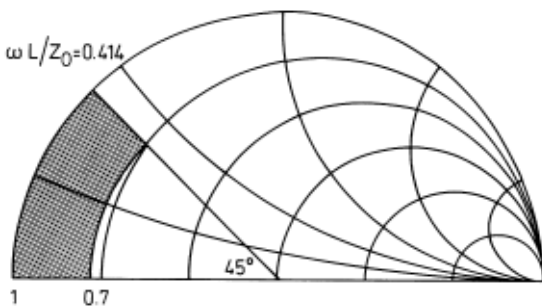


Fig.6 Smith chart showing the region (shaded) where the positions of the return loss minima are independent of k_1 , k_2 and L_1

4.2.1 Investigation of f_{min_1} and f_{min_2} : First the effect of k_1 , k_2 and L_1 on f_{min_1} and f_{min_2} is investigated. Having run the computer model for various values of k_1 , k_2 and L_1 while monitoring the values of f_{min_1} and f_{min_2} , it is concluded that the positions of the minima of the return loss D , i.e. f_{min_1} and f_{min_2} , are independent of k_1 , k_2 and L_1 given that k_1 , k_2 and L_1 are sufficiently small. On the Smith chart, when the impedance loci are confined within the shaded area of Fig. 6, as f_1 and f_2 are varied, then the positions of the minima f_{min_1} and f_{min_2} stay constant to within 1% irrespective of the values of k_1 , k_2 and L_1 . Small values of k_1 , k_2 and L_1 means that the launching coil has negligible interference on the circuits to be analysed. This can be achieved in practical terms by inserting a coil of small

inductance into the tank circuit, having it connected to the NA to monitor the impedance loci, and changing its position until its coupling factors relative to the tank and applicator circuits become sufficiently small to satisfy the above condition.

Once this has been established and values for k_1 , k_2 and L_1 have been chosen, they can be kept constant without affecting the generality of the results that follow. The next step is to find out how f_{min_1} and f_{min_2} change as functions of f_2 , k and Q_2 . The model parameters used are shown in Table 1.

Table 1: Model parameter ranges for investigation of f_{min_1} and f_{min_2}

f_1	15MHz
Q_1	100-1000
L_1	1 μ H
f_2	12-18MHz
Q_2	10-500
L_2	1 μ H
$k^2 Q_1 Q_2$	0.1-1000
k_1	0.025
k_2	0.01
L_1	0.1 μ H

The positions of the minima f_{min_1} and f_{min_2} are plotted against f_2 for various values of $k^2 Q_1 Q_2$, as shown in Fig. 7, Q_2 being kept constant. One return loss minimum closely follows f_2 while the other minimum stays close to f_1 . Now as $k^2 Q_1 Q_2$ increases the separation between the two minima increases. When coupling is greater than critical the two minima do not overlap. For coupling less than critical, the two minima are at the resonant frequencies of the two circuits. It is further observed that the separation between the minima decreases as f_2 approaches f_1 .

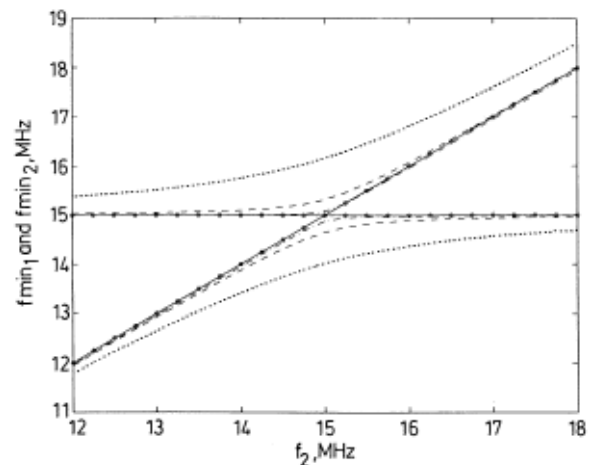


Fig.7 Plot of f_{min_1} and f_{min_2} against f_2 for various values of $k^2 Q_1 Q_2$
 $f_1 = 15$ MHz, $Q_1 = 500$ and $Q_2 = 100$
 ○ 0.1
 — 1.0
 - - - 10
 . . . 100
 ····· 1000

Fig. 8 shows a plot of the separation of the minima ($f_{min_2} - f_{min_1}$) against f_2 for various values of $k^2 Q_1 Q_2$ with Q_2 being kept constant. It is clear that as f_2 approaches f_1 the separation between the two minima decreases. Further, ($f_{min_2} - f_{min_1}$) is always minimum when $f_2 = f_1$, which is the condition for maximum effi-

ciency. So a method of matching the applicator to the tank circuit would be to minimise the separation between the two minima of the return loss D . Furthermore, it has been observed that by plotting (f_{min_2}/f_{min_1}) instead of their difference, this ratio is also minimum when $f_2 = f_1$, and if $\log [\min(f_{min_2}/f_{min_1})]$ is plotted against k for various values of Q_2 and f_1 , as shown in Fig. 9 it is observed that both f_1 and Q_2 have practically no effect on $\log [\min(f_{min_2}/f_{min_1})]$. The model was also run for different values of Q_1 giving the same results. Therefore by measuring f_{min_1} and f_{min_2} when their separation is minimum these curves can be used to obtain the coupling factor k . This result is independent of the resonant frequencies of the coupled circuits and of their Q-factors. There will be some small errors, however, when the Q-factors differ by more than an order of magnitude.

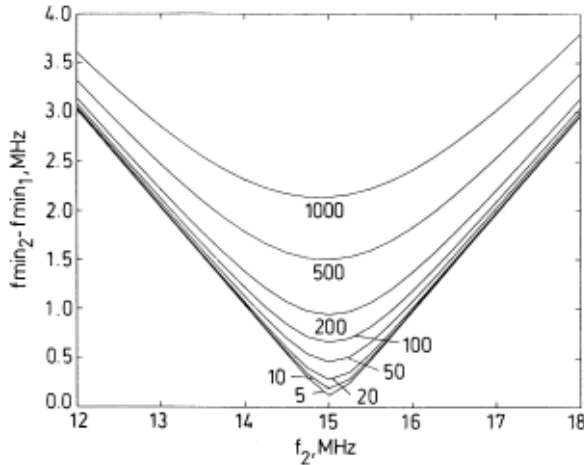


Fig. 8 Plot of $f_{min_2} - f_{min_1}$ against f_2 for various values of $k^2 Q_1 Q_2$ $f_1 = 15\text{MHz}$, $Q_1 = 500$ and $Q_2 = 100$

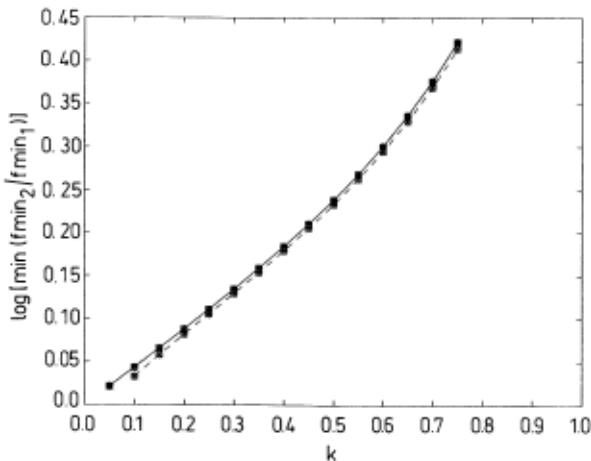


Fig. 9 Plot of $\log[\min(f_{min_2}/f_{min_1})]$ against k for various values of Q_2 and f_1
 $Q_1 = 500$, $f_1 = 0.01 - 100\text{MHz}$
 --- $Q_2 = 10$
 $Q_2 = 50$
 - - - $Q_2 = 100$
 ——— $Q_2 = 500$
 ● $f_1 = 10\text{kHz}$
 ○ $f_1 = 100\text{kHz}$
 × $f_1 = 1\text{MHz}$
 + $f_1 = 10\text{MHz}$
 * $f_1 = 100\text{MHz}$

4.2.2 Investigation of D_{min_1} and D_{min_2} : Now that the coupling factor k can be obtained from f_{min_1} and f_{min_2} , the product $Q_1 Q_2$ is needed to calculate the power efficiency of the circuit using eqn. 18. One needs to study the values of D_{min_1} and D_{min_2} which are related to the Q-factors of the circuits and to the coupling factors of the launching coil to these circuits.

Fig. 10 shows a plot of D_{min_1}/D_{min_2} against f_2 for various values of $k^2 Q_1 Q_2$ when $k_2 = 0$. In Section 4.2.1

it was found that operating within the shaded area shown in Fig. 6 renders the value of k_2 irrelevant. It can be seen that the values of the two peaks become approximately equal when $f_2 = f_1$. It is further observed that as $k^2 Q_1 Q_2$ increases D_{min_1} and D_{min_2} become more comparable. Moreover, by plotting D_{min_1}/D_{min_2} against f_2 for various values of Q_2 it can again be observed that as Q_2 decreases the values of D_{min_1} and D_{min_2} become closer. Finally, D_{min_1}/D_{min_2} is plotted against f_2 for various values of k_2/k_1 as shown in Fig. 11. It can be seen that the minima are not equal at optimum matching (which occurs at $f_1 = f_2$). Therefore, when trying to match the system using the NA one should ignore the size of the minima and concentrate only on their separation.

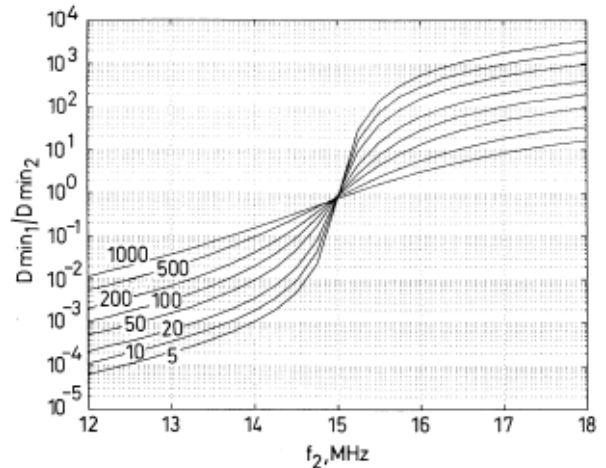


Fig. 10 Plot of D_{min_1}/D_{min_2} against f_2 for various values of $k^2 Q_1 Q_2$ $f_1 = 15\text{MHz}$, $Q_1 = 500$ and $Q_2 = 100$

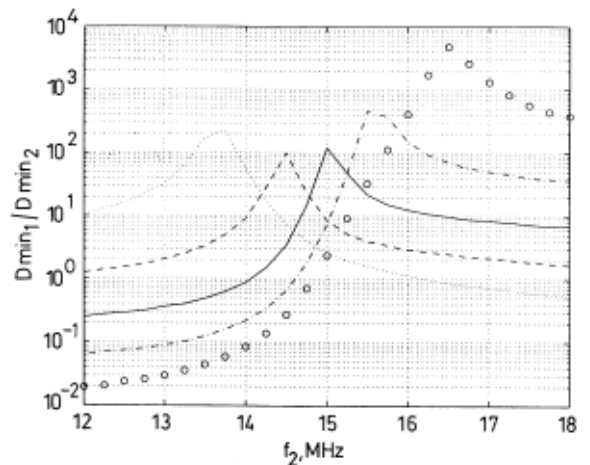


Fig. 11 Plot of D_{min_1}/D_{min_2} against f_2 for various values of k_2/k_1 $f_1 = 15\text{MHz}$, $Q_1 = 500$, $Q_2 = 100$ and $k^2 Q_1 Q_2 = 100$
 ○ 0.25
 - - - 0.5
 ——— 1.0
 - - - 2.0
 4.0

The model has been run with various values of the parameters stated in eqn. 23. However, no simple relation between D_{min_1} , D_{min_2} and $k^2 Q_1 Q_2$ or Q_1 or Q_2 has been identified. Therefore a more mathematical approach, which follows, is necessary.

5 Method for estimation of coupled circuits parameters using the network analyser

Maximum coupling efficiency occurs when $\omega_0 = \omega_1 = \omega_2$. From eqns. 3 and 4 the impedances of the two res-

onant circuits at this condition become $Z_1(\omega_0) = R_1$ and $Z_2(\omega_0) = R_2$. The impedance seen by the NA given by eqn. 22 at angular frequency ω_0 is given by

$$\begin{aligned} Z_{NA}(\omega_0)|_{(\omega_1=\omega_2)} &= R_l + j\omega_0 L_l \\ &+ \frac{\omega_0^2 M_1^2 R_2 - 2j\omega_0^3 M_1 M_2 M + \omega_0^2 M_2^2 R_1}{\omega_0^2 M^2 + R_1 R_2} \\ &= R_l + \omega_0 L_l + \left[\frac{k_1^2 Q_1 + k_2^2 Q_2}{1 + k^2 Q_1 Q_2} \right. \\ &\quad \left. + j \left(1 - \frac{2k_1 k_2 k Q_1 Q_2}{1 + k^2 Q_1 Q_2} \right) \right] \quad (24) \end{aligned}$$

This equation will be used below to calculate $k^2 Q_1 Q_2$.

The system becomes detuned by changing the resonant frequency of the applicator ω_2 . If ω_2 moves sufficiently far away from ω_1 , so that the minima of the return loss do not change in shape but only move away from each other, then the impedance seen by the NA at ω_1 given by eqn. 22 can be approximated by

$$\begin{aligned} Z_{NA}(\omega_1)|_{(\omega_1 \neq \omega_2)} &= R_l + j\omega_1 L_l + \frac{\omega_1^2 M_1^2}{R_1} \\ &= R_l + \omega_1 L_l [k_1^2 Q_1 + j] \quad (25) \end{aligned}$$

where ($\omega_1 \neq \omega_2$) signifies this de-tuned condition, since the applicator circuit impedance does not have an appreciable effect close to ω_1 . The same applies for the impedance at ω_2 yielding

$$\begin{aligned} Z_{NA}(\omega_2)|_{(\omega_1 \neq \omega_2)} &= R_l + j\omega_2 L_l + \frac{\omega_2^2 M_2^2}{R_2} \\ &= R_l + \omega_2 L_l [k_2^2 Q_2 + j] \quad (26) \end{aligned}$$

Q_2 in the detuned condition is assumed to be approximately the same as when the system is tuned especially for loaded applicators.

Using these results a method of rapid estimation of the coupled circuits parameters using the NA is formulated as follows:

- (i) Using the method outlined in the previous section the system is tuned for maximum efficiency and the coupling factor k is obtained
- (ii) The frequency of operation f_0 can be estimated by averaging f_{min_1} and f_{min_2} when the distance between them is at a minimum
- (iii) Without disturbing the system (i.e. $f_1 = f_2 = f_0$) the impedance $Z_{NA}(\omega_0)|_{(\omega_1=\omega_2)}$ is measured directly using the NA. Also the resistance R_l of the launching coil can be measured directly using the NA at a frequency far away from f_0 where the coupled circuits have no effect on the impedance seen by the NA
- (iv) The system is then detuned by changing the plate separation so that the minima of the return loss do not change in shape but only move relatively to each other ($\omega_1 \neq \omega_2$)
- (v) When the resonant frequencies are far apart the minima in the return loss D will be situated at these frequencies, i.e. $f_{min_1} = f_1$ and $f_{min_2} = f_2$
- (vi) Then the impedances at the two minima of the return loss are measured using the NA. These are equal to $Z_{NA}(\omega_1)|_{(\omega_1 \neq \omega_2)}$ and $Z_{NA}(\omega_2)|_{(\omega_1 \neq \omega_2)}$. Using eqns. 25 and 26 L_l , $k_1^2 Q_1$ and $k_2^2 Q_2$ can be easily obtained
- (vii) Finally $k^2 Q_1 Q_2$ is obtained from $Z_{NA}(\omega_0)|_{(\omega_1=\omega_2)}$ using eqn. 24.

6 Verification of the method

The experimental method described above is used to derive the operating parameters of a 13.56MHz, 1.5kW laboratory RF system. The applicator is loaded with a wet paper block of dimensions 456mm \times 114mm \times 14mm. Its dry weight is 243g and its wet weight is 593g, representing a moisture content of about 144% on a dry weight basis. This is taken to represent the average moisture content within the applicator when operating under steady state conditions.

First, a launching coil of low inductance is constructed and placed inside the tank circuit so that the conditions described in Section 4.2.1 are satisfied. Then the applicator is tuned for maximum efficiency by minimising the separation between the minima in the return loss using a commercially available NA, model HP8753C. Their positions are noted to be $f_{min_1} = 13.504$ MHz and $f_{min_2} = 13.722$ MHz. Taking the logarithm of (f_{min_2}/f_{min_1}) one obtains that $\log[\min(f_{min_2}/f_{min_1})] = 0.00695$. This value is rather low and the corresponding value of k cannot be obtained from Fig. 9. However, by fitting a line through it for small values of k the following expression is derived:

$$k = \ln \left[\min \left(\frac{f_{min_2}}{f_{min_1}} \right) \right] \quad (27)$$

Using the above equation one obtains $k = 0.016$.

One then proceeds by estimating the frequency of operation by averaging f_{min_1} and f_{min_2} when the distance between them is minimum and the impedance at this frequency is measured. The values are $f_0 = 13.613$ MHz and $Z_{NA}(\omega_0)|_{(\omega_1=\omega_2)} = 1.36 + j17.26\Omega$. Also the resistance of the launching coil is measured to be $R_l = 0.22\Omega$.

The system is then detuned by changing the plate separation and the two impedances $Z_{NA}(\omega_1)|_{(\omega_1 \neq \omega_2)}$ and $Z_{NA}(\omega_2)|_{(\omega_1 \neq \omega_2)}$ are measured. The values are $f_1 = 13.603$ MHz, $Z_{NA}(\omega_1)|_{(\omega_1 \neq \omega_2)} = 19.46 + j16.43\Omega$, $f_2 = 16.0$ MHz and $Z_{NA}(\omega_2)|_{(\omega_1 \neq \omega_2)} = 0.66 + j2.22\Omega$. Using eqn. 25 $L_l = 192.2$ nH and $k_1^2 Q_1 = 1.171$. Using eqn. 26 $L_l = 221.0$ nH and $k_2^2 Q_2 = 0.020$. Finally using eqn. 24 and $L_l = 206.6$ nH, the average of the two values found above, the parameter $k^2 Q_1 Q_2$ is calculated and found equal to 17.46.

Table 2: Circuits parameter values obtained using fast estimation and nonlinear minimisation methods

	Fast estimation	Nonlinear minimisation	Difference (%)
R_l (Ω)	0.22	0.23	4.3
L_l (nH)	206.6	220.24	6.2
$k_1^2 Q_1$	1.171	1.075	8.9
$k_2^2 Q_2$	0.020	0.018	11.1
k	0.016	0.018	11.1
$k^2 Q_1 Q_2$	17.46	17.56	0.6
f_0 (MHz)	13.613	13.622	0.06
η (%)	94.58	94.61	0.03

The same parameters are deduced using the nonlinear minimisation method as described in [4]. The parameters found at optimum matching are $L_l = 220.24$ nH, $k_1^2 Q_1 = 1.075$, $k_2^2 Q_2 = 0.018$, $k = 0.018$, $k^2 Q_1 Q_2 = 17.56$. Further, $f_1 = 13.617$ MHz and $f_2 = 13.626$ MHz which are approximately equal, showing

that the method for tuning the system is valid. The parameters deduced using both methods are summarised in Table 2. It can be seen that the parameter values obtained using the rapid estimation method are good approximations to those obtained by the more accurate but laborious nonlinear minimisation method. For this system the power transfer efficiency is given by substituting the value of $k^2 Q_1 Q_2$ into eqn. 18 to yield a value of 94.6%.

7 Conclusions

A method of tuning high power RF processing systems using a network analyser to attain maximum power transfer efficiency conditions is presented. Using a computer model a thorough analysis of various possible systems is made and the method is generalised so that it is applicable to any system. This method is based simply on minimising the separation between the two minima of the return loss seen by the launching coil. Finally, a fast way of obtaining the operating parameters and the power transfer efficiency of a system is outlined. The experimental results are compared to the more accurate nonlinear minimisation method showing very good overall agreement with a maximum difference of about 11% between the two. The advantage of the new method is that it is much faster and simpler than existing methods and avoids characterisation of systems based on intuition.

8 References

- 1 JONES, P.L.: 'Radio frequency processing in Europe', *J. Microw. Power Electromagn. Energy*, 1987, 22, (3), pp. 143-153
- 2 METAXAS, A.C.: 'Foundations of electroheat, a unified approach' (Wiley, 1996)
- 3 METAXAS, A.C.: 'The dynamic impedance of radio frequency heating generators', *J. Microw. Power Electromagn. Energy*, 1987, 22, (3), pp. 127-136
- 4 NEOPHYTOU, R.I., and METAXAS, A.C.: 'Computer simulation of a radio frequency industrial system', *J. Microw. Power Electromagn. Energy*, 1996, 31, (4), pp. 251-259
- 5 METAXAS, A.C.: 'Network analysis on radio frequency prototype industrial applicators', *J. Microw. Power*, 1985, 20, (4), pp. 197-216

- 6 PERKIN, R.M.: 'The modelling of radio frequency coupled circuits', *J. Microw. Power Electromagn. Energy*, 1987, 22, (3), pp. 137-142
- 7 METAXAS, A.C., and CLEE, M.: 'Coupling and matching of radio frequency industrial applicators', *Power Eng. J.*, 1993, 7, (2), pp. 85-93
- 8 CHAFFEE, E.L.: 'Theory of thermionic vacuum tubes' (McGraw-Hill, 1933), Chap. 14
- 9 REICH, H.J.: 'Functional circuits and oscillators' (Van Nostrand, 1961), Chap. 82
- 10 'Matlab user's guide' (The MathWorks, Inc., 1992)

9 Appendix: Derivation of Z_{NA} when launching coil interacts with both resonant circuits

For the system shown in Fig. 2b one has the following equations:

$$0 = Z_1 I_1 + j\omega M I_2 + j\omega M_1 I_l \quad (28)$$

$$0 = Z_2 I_2 + j\omega M I_1 + j\omega M_2 I_l \quad (29)$$

$$V_l = (R_l + j\omega L_l) I_l + j\omega M_1 I_1 + j\omega M_2 I_2 \quad (30)$$

Using eqns. 28 and 29, I_1 and I_2 are obtained as functions of I_l

$$I_1 = -\frac{\omega^2 M_2 M + j\omega M_1 Z_2}{\omega^2 M^2 + Z_1 Z_2} I_l \quad (31)$$

$$I_2 = -\frac{\omega^2 M_1 M + j\omega M_2 Z_1}{\omega^2 M^2 + Z_1 Z_2} I_l \quad (32)$$

Substituting eqns. 31 and 32 in eqn. 30 one obtains

$$V_l = \left[R_l + j\omega L_l - \frac{j\omega M_1 (\omega^2 M_2 M + j\omega M_1 Z_2)}{\omega^2 M^2 + Z_1 Z_2} - \frac{j\omega M_2 (\omega^2 M_1 M + j\omega M_2 Z_1)}{\omega^2 M^2 + Z_1 Z_2} \right] I_l \quad (33)$$

Therefore the impedance seen by the network analyser is given by

$$Z_{NA} = R_l + j\omega L_l + \frac{\omega^2 M_1^2 Z_2 - 2j\omega^3 M_1 M_2 M + \omega^2 M_2^2 Z_1}{\omega^2 M^2 + Z_1 Z_2} \quad (34)$$